On the minimal model for the low frequency wobbling instability of friction discs

Alexander Fidlin, Olga Drozdetskaya, Bernd Waltersberger

Accepted Manuscript

Title: On the minimal model for the low frequency wobbling instability of friction discs

Authors: Alexander Fidlin, Olga Drozdetskaya, Bernd Waltersberger

PII: S0997-7538(11)00043-X

DOI: 10.1016/j.euromechsol.2011.03.009

Reference: EJMSOL 2695

To appear in: *European Journal of Mechanics / A Solids*

Received Date: 10 January 2011

Revised Date: 19 March 2011

Accepted Date: 23 March 2011

Please cite this article as: Fidlin, A., Drozdetskaya, O., Waltersberger, B. On the minimal model for the low frequency wobbling instability of friction discs, European Journal of Mechanics / A Solids (2011), doi: 10.1016/j.euromechsol.2011.03.009

On the minimal model for the low frequency wobbling instability of friction discs

Alexander Fidlin*, Olga Drozdetskaya**, and Bernd Waltersberger***

*Karlsruhe Institute of Technology,Kaiserstr. 10, D-76131, Germany

**LuK GmbH & Co. KG, Industriestr. 3, D-77815, Buehl, Germany

***University of Applied Sciences Offenburg, Badstraße 24, D-7652, Offenburg, Germany

Summary. An analytical and numerical study of the wobbling dynamics of friction disks is presented. Of particular interest is the excitation mechanism taking into account two contrarian effects both originating in dry friction: the circulatory terms describing the energy input due to the sliding contacts and the friction induced damping which stabilizes the system. Balance of these terms determines the instability domain in the parameter space. It is shown that there is a slip threshold so that, if the slip is under this limit, the system remains stable. If the slip is larger than this limit then the criterion of stability is determined by the relation between the friction coefficient and the internal damping. The limit cycle appearing in the unstable domain is also investigated. It is shown that the limit cycle can be described as a kind of a regular reverse precession of the wobbling disc. Its amplitude is limited by the geometric nonlinearity and partial contact loss. Analytic results are compared with numeric simulations.

Keywords: Friction disc, wobbling, instability, limit cycle, contact loss

1. Introduction

Wobbling plates is a fascinating research object. Even the simplest case of a free disc still attracts attention of physicists and teachers [1, 2] and demonstrates an inspiring variety of effects in its dynamic behavior. Although friction discs are quite usual in technical applications, their dynamics didn't attract much attention in the past. Dry and wet friction clutches in automotive transmissions [3, 4] can be mentioned here alongside with clutch actuation bearings [5]. Great attention was paid in the past to the various dynamic phenomena in the slider – disk contact [6 – 11]. The main applications here are the standard test rigs for measurement of the friction coefficient [8], friction brakes [10] and magnetic disk drives [9]. Various instabilities usual in automotive drive trains can be split at least into two groups. Phenomena related with the properties in the tribological contact (first of all with the effect of the sliding speed, temperature and contact pressure on the friction coefficient) belong to the first one. The second group contains effects depending mainly on the level of friction force and not on its gradient. The simplest one is the radial instability of friction discs described in [12 – 14]. The second one is the mode coupling which was investigated extensively in connection with the break squeal problem [15 – 18]. The models [15] and [17] are quite general and mainly oriented on the principal effect of the non-symmetric stiffness matrix generated through friction forces. The models [16] and [18] are more specific and concentrated on specific properties of the brake, i.e. wobbling instability generated by the two sided point contact between the pads and the disk. Gyroscopic terms and friction induced damping were also taken into account alongside with the non-symmetric stiffness for this particular case of the brake in [18].

Whereas so much attention was paid to the brake squeal, much less efforts were invested in the analysis of the instabilities in the clutches and the other friction discs. The main difference between brakes and friction discs is the fact that the friction contact in last ones is distributed completely symmetrically along a circle. Another difference is connected with the

rotation of both friction disc and the elastic pad. This principal effect that the friction instability in such a system can be caused through the mode coupling was discussed in [19]. The specific skew-symmetry of the stiffness matrix allows here to obtain very simple analytic expressions for the boundaries of the stability domain. It was later investigated in a more accurate way in [20], where gyroscopic terms were taken into account. However in both publications [19, 20] an important effect of the friction forces which are not only the source of the circulatory terms destabilizing the disc but also generate the friction induced damping acting alongside with the structural damping as an additional source of stability was omitted. Another example of a quite artificial system generating a completely skew-symmetric stiffness matrix was investigated in [21]. The analysis was accomplished by the nonlinear stick-slip phenomena which enabled the authors to obtain the approximate predictions for the amplitude of the limit cycle. However the friction induced damping couldn't occur there due to the one-dimensional contact description.

The wobbling instability of friction discs with the one side contact distributed along a circle is consequently investigated in the present paper. Based on the complete nonlinear equations of motion (section 2) we take into account all the terms appearing in the linear approximation (section 3): structural stiffness and damping, gyroscopic terms, the friction induced circulatory matrix and the friction induced damping. The source of the friction induced damping is explained in section 3.1 on a simple example of a mass on a sliding belt. The effects of different design parameters are analyzed in section 3.2. Closed analytic predictions for the boundaries of the stability domain are presented. Then the nonlinear effects are investigated in section 4. It is shown that the described instability leads to the classic transcritical bifurcation. The amplitude of the limit cycle can be easily predicted, if one takes the geometric nonlinearity into account. However this prediction is valid only for extremely small amplitudes of the limit cycle, i.e. in the vicinity of the bifurcation point. The further development of the nonlinear dynamics of the system is accompanied by the partial loss of contact between the friction disc and the rotating master disc. The corresponding limit cycle (both without and with contact loss) can be described as a kind of regular precession directed against the main sliding. All analytic results are compared with the numeric simulations of the nonlinear system which were performed with the simulation software DynaReg2D [14, 22].

2. Friction disc and its equations of motion

Consider the system in Fig. 1 representing a rotating disc on an elastic pad.

The disc rotates around its symmetry axis with a given constant velocity $\dot{\varphi}$ and can tilt together with the bar which has its fixed point in the ball joint. The length of the bar is h. The disc contacts with the friction ring of radius R which is mounted on the elastic layer of a certain stiffness c. This compliance represents the properties of the friction material at the interface between the clutch discs. Sometimes additional axial springs are used in the clutch disc design in order to assure the soft contact. In that case the stiffness distribution is not completely uniform in circumferential direction. However this non-symmetry could cause some additional excitation of a higher order which is not of the main interest in the present paper.

The distance between the ball joint and the unloaded position of the friction ring is H. It means the difference $(h-H)$ multiplied by the layer's stiffness determines the preload of the system. ω is the rotation speed of the friction ring around the fixed vertical axis which is also assumed to be constant. The coupling between the disc and the friction ring is described by Coulomb's friction law with the friction coefficient μ and the normal load determined by the layer's stiffness and its deformation.

In order to obtain the equations of motion we introduce two coordinate systems. The first one $(\vec{e}_x, \vec{e}_y, \vec{e}_z)$ is fixed in the inertial space. The second one $(\vec{i}, \vec{j}, \vec{k})$ is semi connected with the friction disc. It means these vectors tilt together with the body (friction disc) but don't rotate with the velocity $\dot{\varphi}$. The relationship between these coordinate systems can be described by the corresponding rotation matrix.

$$\begin{aligned}
\vec{e}_x &= \vec{i}\cos\beta + \vec{k}\sin\beta \\
\vec{e}_y &= \vec{i}\sin\alpha\sin\beta + \vec{j}\cos\alpha - \vec{k}\sin\alpha\cos\beta \\
\vec{e}_z &= -\vec{i}\cos\alpha\sin\beta + \vec{j}\sin\alpha + \vec{k}\cos\alpha\cos\beta
\end{aligned} \tag{1}$$

The angular speed of the disc and the equations of motion can be obtained as follows:

$$\vec{\omega}_S = \dot{\alpha}\vec{e}_x + \dot{\beta}\vec{j} + \dot{\varphi}\vec{k} = \vec{i}\,\dot{\alpha}\cos\beta + \vec{j}\,\dot{\beta} + \vec{k}\,(\dot{\varphi} + \dot{\alpha}\sin\beta) \tag{2}$$

$$\vec{L} = \vec{\vec{I}} \cdot \vec{\omega}_S \tag{3}$$

$$\dot{\vec{L}} = \vec{M} \tag{4}$$

Here $\vec{\vec{I}} = J_\alpha \vec{i}\,\vec{i} + J_\beta \vec{j}\,\vec{j} + J\vec{k}\,\vec{k}$ is the inertia tensor of the disc with the rod. Equation (2) is based on the modeling assumption that any desired angular velocity component $\dot{\varphi}\vec{k}$ can be maintained by an external torque vector that is always parallel to $\vec{k}$.

In order to calculate the external torque we assume that the contact takes place along the circle line:

$$\vec{r}_A = R\cos\psi\vec{i} + R\sin\psi\vec{j} + h\vec{k} \tag{5}$$

Here ψ is an angle along the contact circle. The torque is generated by two different sources. Firstly it is the reaction force of the elastic layer under the friction ring. Secondly it is the friction force between the disc and the ring. We assume here that the rotation speeds ω and $\dot{\varphi}$ are significantly different and thus there is permanent slip in the contact. In order to calculate the elastic force we assume that it depends only on the vertical deformation of the layer (along the vector $\vec{e}_z$) and is directed along the body frame axis $\vec{k}$. (The friction ring is assumed rigid.) Then the force generated by a certain element of the elastic layer is

$$d\vec{F}_e = -c(\vec{r}_A \cdot \vec{e}_z - H)\frac{d\psi}{2\pi}\vec{k} = \frac{c}{2\pi}(H - h\cos\alpha\cos\beta - R\sin\psi\sin\alpha + R\cos\psi\cos\alpha\sin\beta)\vec{k}\,d\psi \tag{6}$$

In order to calculate the friction force we need the velocity of each point along the contact line. The velocity of the point *A* of the disc which is determined by the vector $\vec{r}_A$ is

$$\vec{V}_A = \vec{\omega}_S \times \vec{r}_A = (\dot{\beta}h - \dot{\varphi}R\sin\psi)\vec{i} + (\dot{\varphi}R\cos\psi - \dot{\alpha}h)\vec{j} + (\dot{\alpha}R\sin\psi - \dot{\beta}R\cos\psi)\vec{k} \tag{7}$$

The velocity of the corresponding point of the friction ring on the elastic pad is

$$\vec{V}_{A\_ring} = \omega\vec{e}_z \times \vec{r}_{Ad} = \omega(h\sin\alpha - R\sin\psi\cos\alpha\cos\beta)\vec{i} + \omega(R\cos\psi\cos\alpha\cos\beta + h\cos\alpha\sin\beta)\vec{j} - \omega(R\cos\psi\sin\alpha + R\sin\psi\cos\alpha\sin\beta)\vec{k} \tag{8}$$

Then the friction force of the same element can be calculated as follows (here and further we assume the Coulomb friction with constant friction coefficient):

$$d\vec{F}_R = -\mu\left|d\vec{F}_e\right|\frac{\vec{V}_r^{\tau}}{\left|\vec{V}_r^{\tau}\right|} \tag{9}$$

Here $\vec{V}_r^{\tau}$ is the tangential component of the relative velocity between the disc and the ring:

$$\vec{V}_r = \vec{V}_A - \vec{V}_{A\_ring};\ \vec{V}_r^{\tau} = \vec{V}_r - (\vec{V}_r \cdot \vec{k})\vec{k} \tag{10}$$

Having the forces we can calculate the elementary torque:

$$d\vec{M} = \vec{r}_A \times \left(d\vec{F}_e + d\vec{F}_R\right) \tag{11}$$

The full torque can be obtained if we integrate the elementary torque along the contact line:

$$\vec{M} = \int_0^{2\pi} d\vec{M} \tag{12}$$

Note that completely closed contact between the discs is assumed here. This assumption will be modified in section 4 in order to obtain the limit cycle with only partial contact.

Relationships(3), (4) and (12) give us finally the required equations of motion.

3. Linearized equations and instability of the sliding disc

Assuming the angles α and β to be small we can linearize the equations of motion which obtain the typical structure:

$$\mathbf{J}\begin{bmatrix}\ddot{\alpha}\\ \ddot{\beta}\end{bmatrix} + (\mathbf{D}+\mathbf{G})\begin{bmatrix}\dot{\alpha}\\ \dot{\beta}\end{bmatrix} + (\mathbf{K}+\mathbf{N})\begin{bmatrix}\alpha\\ \beta\end{bmatrix} = 0 \tag{13}$$

Here **J** is the matrix of inertia, **D** is the symmetric damping matrix, **G** is the skew-symmetric gyroscopic matrix, K is the symmetric stiffness matrix and **N** is the skew-symmetric circulatory matrix. The explicit form of these matrixes can be found in (14) where we suppose that the disc is perfectly symmetric and also introduce *b* as a measure for the structural damping:

$$\mathbf{J}=J_\alpha\begin{bmatrix}1&0\\0&1\end{bmatrix};\ \mathbf{D}=\left(b+\frac{ch^2\mu(h-H)}{2R|\omega-\dot\varphi|}\right)\begin{bmatrix}1&0\\0&1\end{bmatrix};\ \mathbf{G}=J\dot\varphi\begin{bmatrix}0&1\\-1&0\end{bmatrix}$$
$$\mathbf{K}=\frac{1}{2}cR^2\begin{bmatrix}1&0\\0&1\end{bmatrix};\ \mathbf{N}=-\frac{ch\mu R}{2}\left(1-\frac{h(h-H)\omega}{R^2(\omega-\dot\varphi)}\right)\operatorname{sgn}(\omega-\dot\varphi)\begin{bmatrix}0&1\\-1&0\end{bmatrix} \tag{14}$$

These matrices determine the stability of the stationary solution for the friction disc. Due to the modeling assumptions the circulatory matrix is the source of instability. It is proportional to the friction force, which can be easily seen in (14) because this matrix is multiplied by the friction coefficient μ. The physical explanation of this basic effect can be found for example in [15]. However it is not the only matrix proportional to the friction. In the damping matrix **D** we also find such terms. Even more, these terms increase with decreasing slip. These terms describe the friction induced damping. They influence significantly the stability of the friction disc and were unfortunately overlooked in previous publications [15, 16].

3.1. A simple example explaining the appearance of the friction induced damping

In order to reach a better understanding of the friction induced damping let us consider (following to [23]) a simple example of a point mass on a moving belt. However we assume that the mass can move only along the *x* axis perpendicular to the direction of the belt's motion (cf. Fig. 2).

The equation of motion for this mass is quite simple:

$$m\ddot x+cx=-\mu N\cdot\frac{\dot x}{\sqrt{\dot x^2+V^2}} \tag{15}$$

Assuming $\dot x<<V$ we can linearize the friction force on the right hand side and obtain the equation containing the friction induced damping:

$$m\ddot x+\mu N\frac{\dot x}{V}+cx=0 \tag{16}$$

This damping term is quite similar to that in (14) and the belt's velocity plays here the same role like the slip $\omega-\dot\varphi$ in the equations for the friction disc.

Let us now return to the stability conditions for the friction disc.

3.2. Stability conditions for the undamped system

Assuming $b=0$ we introduce the following dimensionless time and parameters:

$$\frac{\omega h(h-H)}{R^2|\omega-\dot\varphi|}=\varepsilon;\ \frac{cR^2}{2}=\tilde c;\ \frac{h\mu}{R}=\tilde\mu;\ \frac{J}{J_\alpha}=I;\ \frac{\tilde c}{J_\alpha}=k^2$$
$$I\frac{\dot\varphi}{k}=p;\ \varepsilon\frac{k}{\omega}=q;\ \operatorname{sgn}(\omega-\dot\varphi)-\varepsilon=s \tag{17}$$
$$\tau=kt\rightarrow(\ )^\bullet=k(\ )'$$

Then we can rewrite the equations (13), (14) as follows:

$$\begin{aligned}&\alpha''+q\tilde\mu\alpha'+p\beta'+\alpha-\tilde\mu s\beta=0\\&\beta''-p\alpha'+q\tilde\mu\beta'+\tilde\mu s\alpha+\beta=0\end{aligned} \tag{18}$$

Now we can calculate the characteristic equation:

$$\det\begin{vmatrix} \lambda^2+\lambda q\tilde{\mu}+1 & \lambda p-\tilde{\mu}s \\ -\lambda p+\tilde{\mu}s & \lambda^2+\lambda q\tilde{\mu}+1 \end{vmatrix} = (\lambda^2+\lambda q\tilde{\mu}+1)^2+(\lambda p-\tilde{\mu}s)^2 = 0. \tag{19}$$

Applying Hurwitz' criterion we get the stability conditions:

$$\begin{aligned} &q > ps \\ &q^2 - qps - s^2 > 0 \end{aligned} \tag{20}$$

Further simplifications are possible if we notice that both p and q are positive. This is obviously the case if the disc and the ring rotate in the same direction. It is usual in almost all sensible applications. Parameter s however can be both positive and negative. We shall distinguish between these two cases.

The solution to (20) is:

$$\begin{aligned} &q > \frac{1}{2}ps\left(1+\sqrt{1+\frac{4}{p^2}}\right) \text{ for } s>0 \\ &q > -\frac{1}{2}ps\left(\sqrt{1+\frac{4}{p^2}}-1\right) \text{ for } s<0 \end{aligned} \tag{21}$$

Returning back to the original parameters the inequalities (21) can be rewritten as follows:

$$\delta\dot{\varphi}\left(1-\frac{cR^2}{J\dot{\varphi}^2\left(\sqrt{1+\frac{2cR^2J_\alpha}{J^2\dot{\varphi}^2}}-1\right)}\right) < \omega-\dot{\varphi} < \delta\dot{\varphi}\left(1+\frac{cR^2}{J\dot{\varphi}^2\left(1+\sqrt{1+\frac{2cR^2J_\alpha}{J^2\dot{\varphi}^2}}\right)}\right) \tag{22}$$

$$\delta = \frac{h(h-H)}{R^2-h(h-H)}$$

It is easy to notice that these inequalities determine the threshold of instability with respect to the slip $(\omega-\dot{\varphi})$. The stability conditions (22) are automatically fulfilled if the slip is sufficiently small and the shape of the threshold depends strongly on the absolute velocity $\dot{\varphi}$. It is also different for the top and the bottom boundaries (the right hand side and the left hand side of the inequalities (22)).

Figure 3 illustrates this behavior and shows the stability boundaries calculated for the following parameter values:

$$\begin{aligned} &R=0.12\,m;\ h=0,15\,m;\ h-H=0.002\,m;\ c=3\cdot10^4\ N/m;\ J=0.04\,kg\cdot m^2 \\ &J_{\alpha0}=0.02\,kg\cdot m^2;\ J_\alpha=J_{\alpha0}+mh^2;\ m=1kg;\ \mu=0,2 \end{aligned} \tag{23}$$

Numeric simulations of the nonlinear equations (3) - (12) were performed with the simulation software DynaReg2D [14, 22]. The stability boundaries were determined numerically by observing the time trajectories over a long period of time. In this particular situation it is not difficult to find the stability boundary because it separates the asymptotically stable and unstable areas. Note that it is not possible to compare analytic and numeric predictions for near-zero slip, because sticking occurs in numeric simulations whereas the permanent slip is

assumed in the analytic model.

There are several peculiarities which have to be mentioned here. Firstly, the domain of small slip between the solid lines is stable. The area of large slip (both positive and negative) corresponds to the instability of the steady state vertical position of the friction disc.

Secondly, the stability domain for the undamped system doesn't depend on the friction coefficient. The reason for this strange feature is the fact that the stability conditions are determined through the balance between the friction induced circulatory terms and also friction induced damping. These terms both are proportional to the friction coefficient. Although the stability conditions (22) are independent from the friction coefficient, the limit case $\mu = 0$ must be excluded from the analysis. It corresponds to the conservative system. Thus the eigenvalues are purely imaginary and no decision on the stability of the system can be made based on the linear approximation.

Thirdly, the geometry of the stability domain depends strongly on the absolute value of the rotation speed $\dot{\varphi}$. Thus these domains for $\dot{\varphi} = 10$ rad/s and for $\dot{\varphi} = 100$ rad/s are quite different.

All these results were overlooked both in [19] and [20], because the stability without any structural damping is possible only due to friction induced damping.

3.3. Stability conditions for the system with structural damping

The performed analysis can be easily generalized for the system in presence of structural damping. Using the signs (17) and introducing additionally $\tilde{b} = b/J_\alpha k$ we can rewrite the equations (13), (14) as follows:

$$\begin{aligned} &\alpha'' + (q\tilde{\mu} + \tilde{b})\alpha' + p\beta' + \alpha - \tilde{\mu}s\beta = 0 \\ &\beta'' - p\alpha' + (q\tilde{\mu} + \tilde{b})\beta' + \tilde{\mu}s\alpha + \beta = 0 \end{aligned} \tag{24}$$

Applying the Hurwitz' criterion to the characteristic equation we obtain the stability conditions:

$$\begin{aligned} &2\tilde{\mu}(q - ps) + \tilde{b} > 0 \\ &\left(\tilde{\mu}q + \tilde{b}\right)\left(2 + \left(\tilde{\mu}q + \tilde{b}\right)^2 + p^2\right)\left(\tilde{b} + \tilde{\mu}q - p\tilde{\mu}s\right) - \left(\tilde{b} + \tilde{\mu}q - p\tilde{\mu}s\right)^2 - \\ &\qquad\qquad \left(\tilde{b} + \tilde{\mu}q\right)\left(1 + \tilde{\mu}^2 s^2\right) > 0 \end{aligned} \tag{25}$$

Let us analyze these inequalities. Consider firstly the case (20), i.e. the undamped system is stable. Then (25) can be transformed to the following form:

$$\tilde{b}^2 + \tilde{b}\tilde{\mu}(2q - ps) + \tilde{\mu}^2(q^2 - qps - s^2) > 0 \tag{26}$$

This inequality is always fulfilled under the above formulated assumptions. Thus damping can not destabilize the disc.

Now let us investigate the case when the undamped system is unstable, i.e.

$$q^2 - qps - s^2 < 0 \tag{27}$$

In that case the inequality (26) can be solved with respect to the friction coefficient:

$$\tilde{\mu} < \frac{\tilde{b}}{s^2 + qps - q^2}\left(q - \frac{ps}{2}\left(1 - \sqrt{1 + \frac{4}{p^2}}\right)\right) \text{ for } s > 0$$
$$\tilde{\mu} < \frac{\tilde{b}}{s^2 + qps - q^2}\left(q - \frac{ps}{2}\left(1 + \sqrt{1 + \frac{4}{p^2}}\right)\right) \text{ for } s < 0 \qquad (28)$$

These relationships show that for each level of friction coefficient there is a certain critical damping. If the damping is below the critical level, the system remains unstable. The disc gets stable if the damping exceeds this level. The last statement can be also inverted. It means for each level of structural damping there is a certain critical friction coefficient. The disc gets unstable if the friction is above this threshold and the slip is sufficiently large. Figure 4 illustrates this fact. It shows the linear dependency between the critical friction and the structural damping. One can also see that the critical friction depends on the sign of the slip. The threshold for the positive slip (the friction ring is faster than the disc) is significantly lower than that for the negative slip (the friction which in that case is necessary for instability is higher). The analytic results corresponding to the relationships (28) correlate quite well with the results of the direct numeric simulations of the full nonlinear system.

Inequalities (28) show that the addiction of the system to instability can be described through the ratio $\tilde{\mu}/\tilde{b}$ for the critical values. This is illustrated in Figure 5.

Consider the synchronization between the disc and the ring. In the simplest case it would mean that the rotation speed of the disc remains constant and the slip decreases continuously towards zero. We assume here that the slip decreases quasi-statically and thus the equations of motion and the obtained stability conditions still hold. Then we can start in the stable domain (solid arrow in Fig. 5) with a large slip. Then we will cross the threshold and come into the unstable area (dashed line). The disc starts to wobble. If we continue to reduce the slip then close to synchronization we will cross the border line for the second time and the system will calm down due to the demonstrated stability for sufficiently small slip (22), (26).

However this screenplay can occur only if the instability wouldn't destroy the system. Thus the nonlinear analysis is necessary in order to estimate the system's behavior in the unstable domain.

Figure 6 shows the main design parameters which can influence the stability of the disc. The first one is the distance between the ball joint and the friction surface (the length of the rod). The longer rod destabilizes the disc. The second one is the stiffness of the elastic layer. Higher stiffness destabilizes the disc.

4. Limit cycle of the wobbling disc due to geometric nonlinearity.

In order to investigate the limit cycle appearing as soon as the friction disc gets unstable and starts to wobble it's necessary to return back to the nonlinear equations. Firstly, we consider equations (1) - (12) taking the first nonlinear terms of the corresponding Taylor's expansions with respect to the tilting angles α, β into account. These can be easily analyzed if one converts from the "Cartesian" angles α, β to the "polar" angles as follows:

$$\alpha = \rho \cos \vartheta,\ \beta = \rho \sin \vartheta \qquad (29)$$

The equations of motion governing α and β differ from (13) due to the nonlinearity in the external torques (the inertial terms don't change in this approximation):

$$\begin{aligned} J_\alpha \ddot{\alpha} + b\dot{\alpha} + J\dot{\varphi}\dot{\beta} &= M_\alpha \\ J_\alpha \ddot{\beta} + b\dot{\beta} - J\dot{\varphi}\dot{\alpha} &= M_\beta \end{aligned} \tag{30}$$

Here M_α and M_β are the components of the full torque vector in (4) calculated along the contact line as shown in (12).

Applying (29) we convert to the new equations governing ρ and ϑ:

$$\begin{aligned} J_\alpha\left(\ddot{\rho} - \rho\dot{\vartheta}^2\right) + b\dot{\rho} + J\dot{\varphi}\rho\dot{\vartheta} &= M_\rho = M_\alpha\cos\vartheta + M_\beta\sin\vartheta \\ J_\alpha\left(\rho\ddot{\vartheta} + 2\dot{\rho}\dot{\vartheta}\right) + b\rho\dot{\vartheta} - J\dot{\varphi}\dot{\rho} &= M_\vartheta = -M_\alpha\sin\vartheta + M_\beta\cos\vartheta \end{aligned} \tag{31}$$

Stationary solutions of these equations can be obtained by setting

$$\dot{\rho} = 0,\ \ddot{\rho} = 0,\ \ddot{\vartheta} = 0,\ \dot{\vartheta} = U \neq 0 \tag{32}$$

The last assumption corresponds to the stationary precession of the friction disc.

The equations determining the stationary solution is:

$$-J_\alpha\rho_{st}U_{st}^{\ 2} + J\dot{\varphi}\rho_{st}U_{st} = M_\rho;\ b\rho_{st}U_{st} = M_\vartheta \tag{33}$$

These equations can be easily solved numerically. There are three sets of stationary solutions. The first one is $\rho = 0$ (and U – undetermined) which corresponds to the investigated equilibrium of the friction disc without tilting. The second and the third one correspond to the regular precession of the tilted disc. However one of these solutions remains unstable, whereas the second one gets stable at the stability boundary of the non-tilted disc. This behavior is illustrated in Fig. 7. Note that there are always two solutions for ρ (positive and negative) describing the same motion. Thus only the positive branch is displayed in the Figure.

Thus we have to deal with the usual transcritical bifurcation for the tilting angle of the friction disc. One can easily find out that the stationary precession's speed U_{st} corresponding to the stable limit cycle is always directed against the slip (cf. the qualitative explanation in [19].

However the described bifurcation doesn't exhaust the complexity of the system's dynamics. The first significant change occurs as soon as the amplitude exceeds the critical level and a part of the disc looses contact to the elastic layer. From now on we will assume that the friction ring is not rigid in the normal direction. It means the ring consists of infinitesimal pads (elastic layer which doesn't transmit normal deformations in tangential direction). Thus the contact between the friction disc and the ring takes place only where the normal springs are loaded. Mathematically this condition can be expressed in terms of the normal force which has to be positive. In such a constellation the equation (12) must be modified. The integration of the forces must be done along the part of the circle with positive normal forces:

$$\vec{M} = \int_{\psi_1}^{\psi_2} d\vec{M} \tag{34}$$

The integration limits ψ_1 and ψ_2 are determined as the solutions of the equation for the normal force:

$$d\vec{F}_e \cdot \vec{k} = \frac{c}{2\pi}(H - h\cos\alpha\cos\beta - R\sin\psi\sin\alpha + R\cos\psi\cos\alpha\sin\beta)\,d\psi = 0 \tag{35}$$

The further analysis can be performed in MAPLE if we apply Taylor's series with respect to angles α and β. However comparison between analytic and numeric predictions shows

that it is necessary to take at least three terms into account in order to achieve an acceptable accuracy (Fig. 8).

The corresponding formulas are so large that their application doesn't give any significant advantage compared with direct numeric simulations. Thus the following results are based on the numeric integration. However the qualitative result can be formulated: The amplitude of the wobbling friction disc is limited due to the partial contact loss between the disc and the layer. The corresponding limit cycle can be described as a direct continuation of the obtained limit cycle with permanent contact. The direction of the precession is opposed to the slip. The described mechanism is completely different to that described in [14]. The nonlinearity limiting the amplitude has nothing to do with the stick-slip effects, but is directly connected with the partial contact loss.

Figure 9 (a) shows the amplitude of the limit cycle as a function of the slip for different rod's lengths. All the simulations were performed with the same parameter values as in (23). It's easy to see that the amplitude of the limit cycle increases with the increasing slip. However the line for $h = 0,2$ is interrupted at a high slip. The reason is that the limit cycle in that domain also gets unstable. This secondary bifurcation is nothing unexpected for such a nonlinear system. It is possible to determine the boundary of the stable limit cycle domain in the parameter space. Figure 9 (b) shows this boundary in the plane "slip over the rod's length" for different angular speeds of the ring. One can notice that the necessary slip decreases with the increasing rod's length. Increasing the absolute rotation speed of the system one increases also the slip which is necessary to destabilize the limit cycle.

Figure 10 shows the development of the instability for consequently increasing values of the slip in the unstable domain. One can see the increasing complexity of the dynamics until something similar to chaotic motion is achieved for the very large slip.

However, these results can be hardly significant (but not impossible) in applications due to extremely large slip. The large slip can occur for example in an automotive clutch with manual transmission due to miss-shift, i.e. if the driver would accidentally engage the reverse gear in a forward driving vehicle.

5. Conclusions

Dynamics of the friction disc is investigated in the article. It is shown that any friction disc tends to wobbling instability. The threshold of the instability is determined by the relationship between the friction induced circulatory terms and damping. The last one contains a structural and a friction induced compounds. The slip between the friction disc and the elastic pad was identified as the principal governing parameter. Without any structural damping there is an instability threshold determined through the sufficiently small slip. If the slip is large, then the system can be always stabilized through the appropriately chosen damping. On the other hand, for any given structural damping the system can get unstable if the slip is not too small and the friction coefficient is sufficiently large. The main design parameters which influence the stability of the friction disc are determined. It is the distance between the ball joint and the friction surface alongside with the slip, the friction coefficient and the stiffness of the underlying elastic layer. Analytic expressions are obtained for the boundaries of the stability domain in the parameter space. These criteria are confirmed through numeric simulations of the complete non-linear system.

A limit cycle appears in the domain of wobbling instability. It occurs due to the geometric nonlinearity of the system. The amplitude of the limit cycle increases while the system penetrates deeper in the unstable domain. With increasing amplitudes the limit cycle leads to the partial contact loss between the friction disc and the underlying elastic layer. It is demon-

strated that also this limit cycle can become unstable. The corresponding motions can be quite complex and even chaotic.

The described model can be considered as the minimal one for the low frequency noise (between 250 and 450 Hz) of the friction discs in automotive clutches. This phenomenon usually called “eek-noise” is a general problem occurring both in manual and double clutch transmissions. The noise appears while shifting, especially during the clutch engagement. The noise can be easily heard by a driver and disappears as soon as the engine is synchronized with the transmission and the clutch is sticking. It is quite difficult to measure the corresponding motion in a vehicle due to the permanent rotation of the clutch and its components. However special measurements on the test rigs with standing clutch and rotating friction disc or vice versa have confirmed the dominating role of the wobbling for the noise generation. The main recommendation to reduce the tilting stiffness of the disc could be also confirmed form the practical point of view. Though the real system is much more complex than the considered one, many additional influences must be taken into account in applications.

Further investigations should be connected with the influences of different types of structural damping. The influence of damping on the stability of circulatory-gyroscopic systems was investigated extensively in [24, 25]. Especially the destabilizing effect of the internal damping both in the elastic layer representing the friction material and in the ball joint could be important for applications. It would be also interesting to investigate dynamics of a disc with two sided frictional contact as well as the friction induced coupling between wobbling and torsional degrees of freedom.

References

[1] R. P. Feynman, 1997. *Surely You’re Joking, Mr. Feynman: Adventures of a Curious Character*, W. W. Norton & Co, 352 p.

[2] S. Tuleja, B. Gazovic, A. Tomori, 2007. Feynman’s wobbling plate, Am. J. Phys. 75 (3), March 2007, pp. 240 – 244.

[3] Reik W.: The Self-Adjusting Clutch, *5th LuK Symposium 1994*, pp. 43 – 63.

[4] Bechart H., Canudas de Wit C., Dolcini P.: Observer-based optimal control of dry clutch engagement. *European Control Conference. CDC-ECC ’05. 44th IEEE Conference on decision and Control*, 2005.

[5] Zink M., Shead R., Welter R.: Clutch release systems, *7th LuK Symposium 2002*, pp. 35 – 47.

[6] Ibrahim R.A.: Friction-induced vibration, chatter, squeal and chaos: Part I – Mechanics of contact and friction, *Appl. Mech. Rev*. 47 (1994) 7, pp. 209 – 226.

[7] Ibrahim R.A.: Friction-Induced Vibration, Chatter, Squeal and Chaos: Part II – Dynamics and Modeling, *Appl. Mech. Rev*. 47 (1994) 7, pp. 227 – 254.

[8] Tworzydlo W.W., Becker E.B., Oden J.T.: Numerical modeling of friction-induced vibrations and dynamic instabilities, *Appl. Mech. Rev*. 47 (1994) 7, pp. 255 – 274.

[9] Honchi M., Kohira H., Matsumoto M.: Numerical simulation of slider dynamics during slider – disk contact, *Tribology International* 36 (2003), pp. 235 – 240.

[10] Wallaschek J., Hach K.-H., Stolz U., Mody P.: A survey of the present state of friction modeling in the analytical and numerical investigation of brake noise generation, *Proceedings of the ASME Vibration Conference, 1999 ASME Design Engineering Technical Conferences*, 12 – 15, 1999, Las Vegas, Nevada

[11] Mottershead J. E., Vibrations and friction-induced instability in discs, in Guran A., Pfeiffer F., Popp K. (Eds.) Dynamics with Friction: Modeling, Analysis and Experiment, Part II, *Series on Stability, Vibration and Control of Systems*, Series B, Vol. 7, World Scientific, 2001, pp. 29 – 74.

[12] A. Fidlin, W. Stamm.: On the radial dynamics of friction discs. *European Journal of Mechanics A/Solids* 28 (2009), pp. 526 - 534.

[13] A. Fidlin, W. Stamm.: On the radial dynamics of friction discs. *Proceedings ENOC 2008, Sixth EUROMECH Nonlinear Dynamics Conference*, St.-Petersburg, Russia, 30 June – 4 July 2008, CD-ROM, 6 p.

[14] W. Stamm, A. Fidlin.: Radial dynamics of rigid friction discs with alternating sticking and sliding. *Proceedings ENOC 2008, Sixth EUROMECH Nonlinear Dynamics Conference*, St.-Petersburg, Russia, 30 June – 4 July 2008, CD-ROM, 6 p.

[15] E. Brommundt.: Ein Reibschwinger mit Selbsterregung ohne fallende Reibkennlinie, *Zeitschrift für Angewandte Mathematik und Mechanik*, 75 (11) 1995, pp. 811 – 820.

[16] K. Popp, M. Rudolph, M. Kröger, M. Lindner.: Mechanisms to generate and to avoid friction induces vibrations, *VDI-Bericht*, Vol. 1736, 2002.

[17] N. Hoffmann, M. Fischer, R. Allgaier, L. Gaul.: A minimal model for studying properties of the mode-coupling type instability in friction induced oscillations, *Mechanics Research Communications*, 29 (2002), pp. 197 – 205.

[18] U. von Wagner, D. Hochlenert, P. Hagedorn.: Minimal models for disk break squeal, *Journal of Sound and Vibration*, 302 (2007), pp. 527 – 539.

[19] A. Fidlin, 2006. *Nonlinear Oscillations in Mechanical Engineering*, Springer: Berlin – Heidelberg, 356 p.

[20] Herve B, Sinou J.-J., Mahe H., Jezequel L.: Analysis of squeal noise and mode coupling instabilities including damping and gyroscopic effects. *European Journal of Mechnaics A/Solids*, 27 (2008), pp. 141 – 160.

[21] J. Kang, Ch. M. Krousgrill, F. Sadeghi.: Oscillation pattern of stick-slip vibrations, *International Journal of Non-Linear Mechanics*, 44 (2009) 7, pp. 820 – 828.

[22] Stamm W., 2011. *Modellierung und Simulation von Mehrkörpersystemen mit flächigen Reibkontakten*. KIT Scientific Publishing, Schriftenreihe des Instituts für Technische Mechanik, Bd. 13, 224 p.

[23] Hochlenert, D., 2006. *Selbsterregte Schwingungen in Scheibenbremsen: Mathematische Modellbildung und aktive Unterdrückung von Bremsenquietschen*. Shaker Verlag, Aachen, 106 p.

[24] Huseyin, K., 1978. *Vibrations and Stability of Multiple Parameter Systems*. Springer Netherlands, 232 p.

[25] Merkin, D. R., 1997. Introduction to the Theory of Stability, Springer, New York, 319 p.

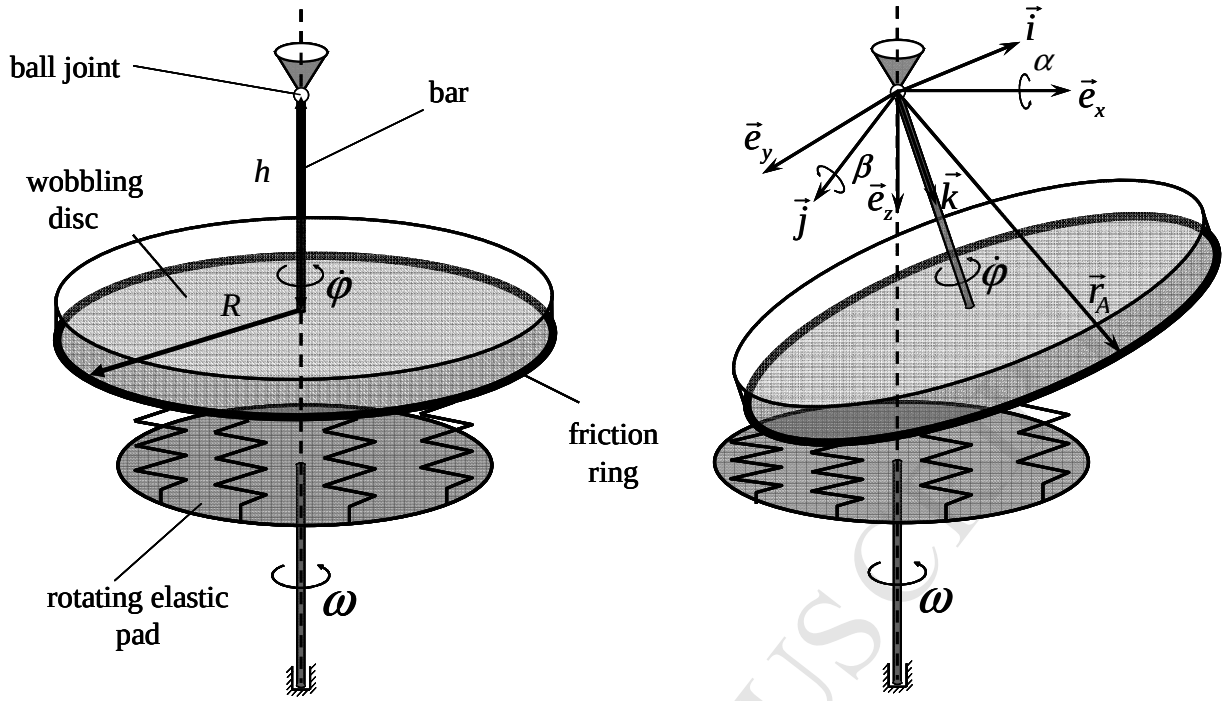

Fig. 1. Rotating friction disc on the elastic pad and the corresponding coordinate systems

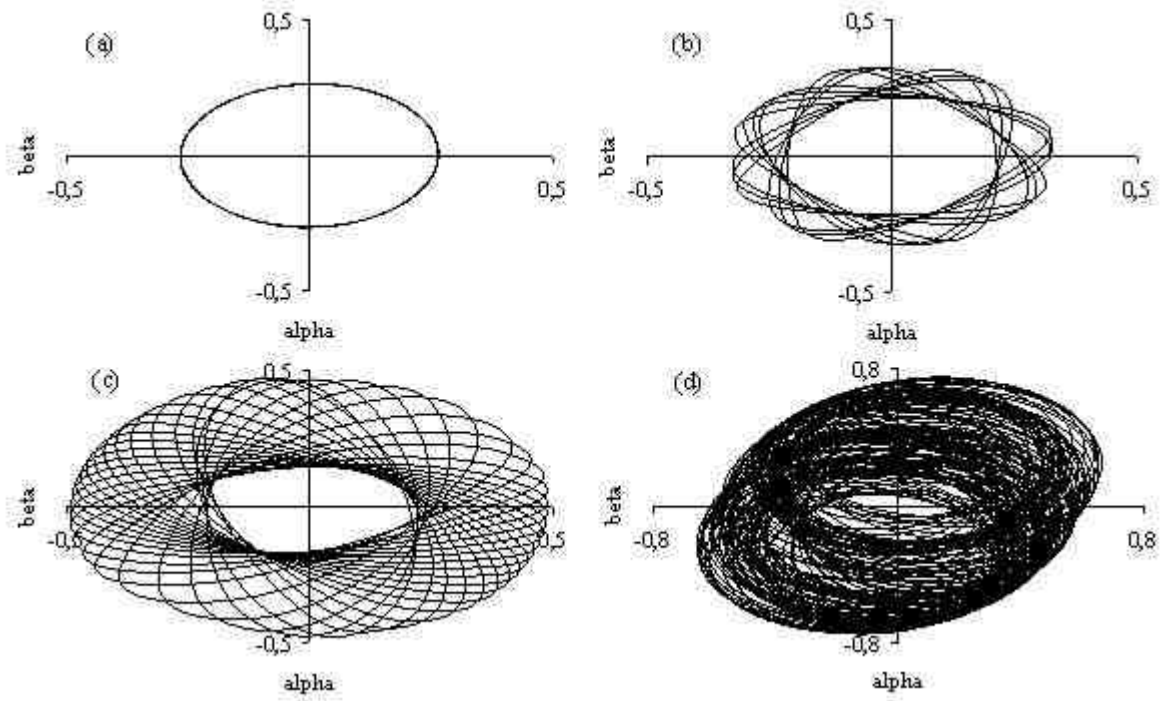

Fig. 10. Limit cycles obtained by numeric simulations: (a) – stable limit cycle with regular precession for the slip $\omega - \dot{\varphi} = 70\,rad/s$, (b) – more complex limit cycle for $\omega - \dot{\varphi} = 75\,rad/s$, (c) – the next complexity level for $\omega - \dot{\varphi} = 105\,rad/s$, (d) – seemingly chaotic behavior for $\omega - \dot{\varphi} = 220\,rad/s$

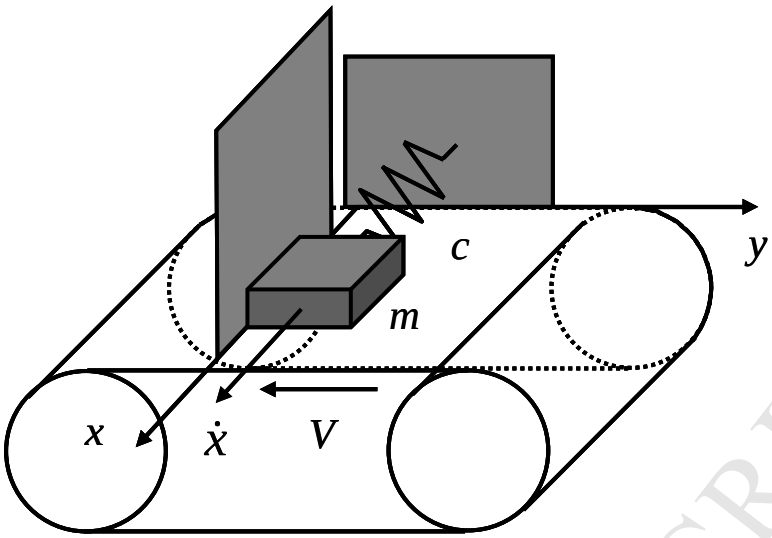

Fig. 2. A mass on the moving belt

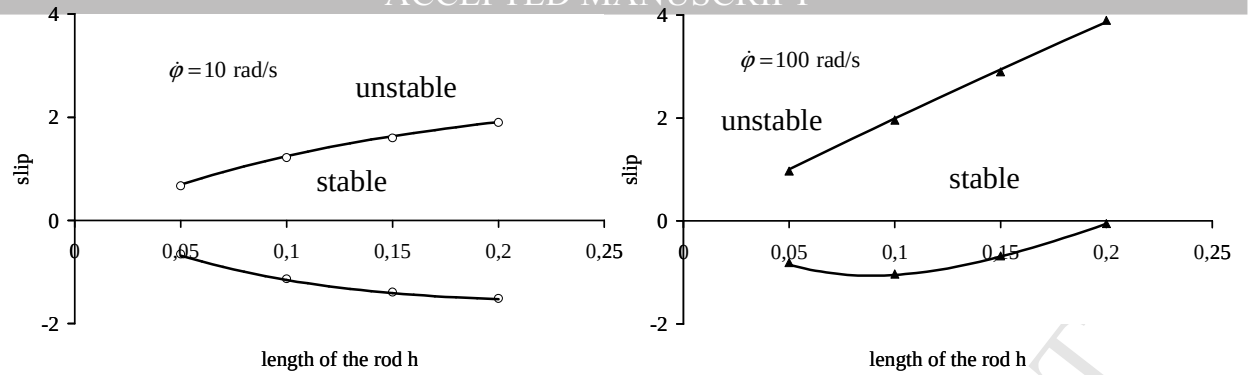

Fig. 3. Stability domain of the undamped system; solid line – stability boundary according to (21), circles/dots – stability boundary according to numeric simulations of the complete equations (3) – (12)

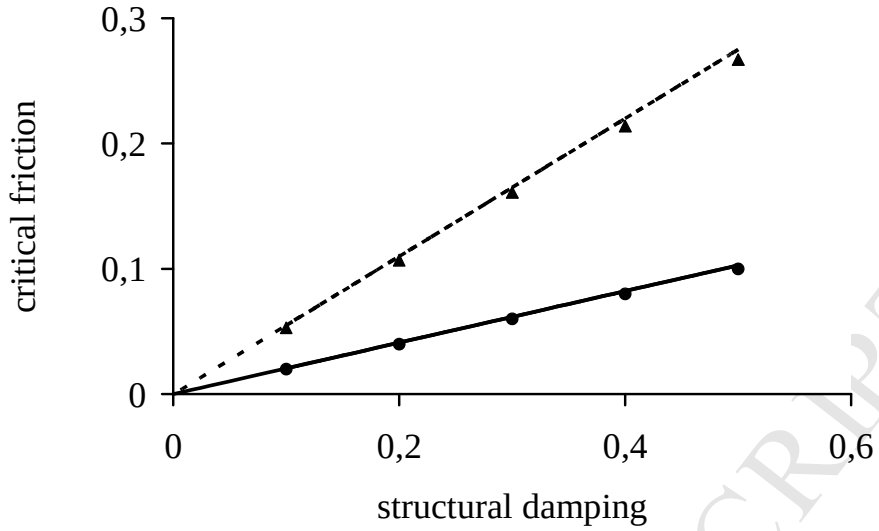

Fig. 4. Critical friction as a function of the structural damping for positive slip (solid line) and negative slip (dashed line); dots and triangles correspond to the numeric simulations of the nonlinear equations

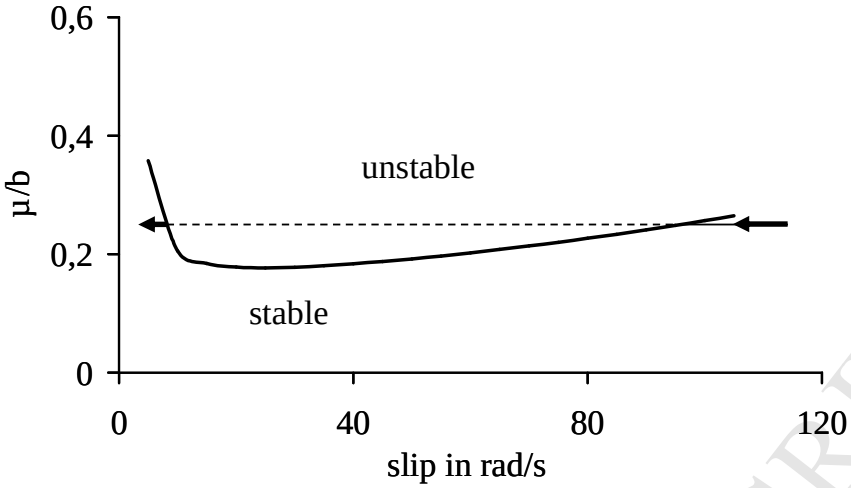

Fig. 5. Alternation of stable and unstable domains while synchronizing the disc

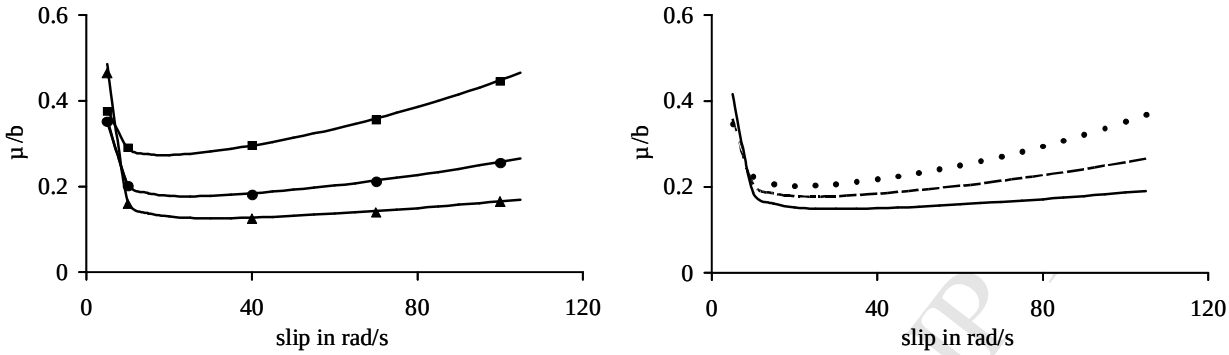

Fig. 6. Friction/damping threshold as a function of the design parameters; (a) h=0,1 for quads, h=0,15 for dots, h=0,2 for triangles; (b) dotted line for c=15.000 N/m, dashed line for c=30.000 N/m, solid line for c=60.000 N/m

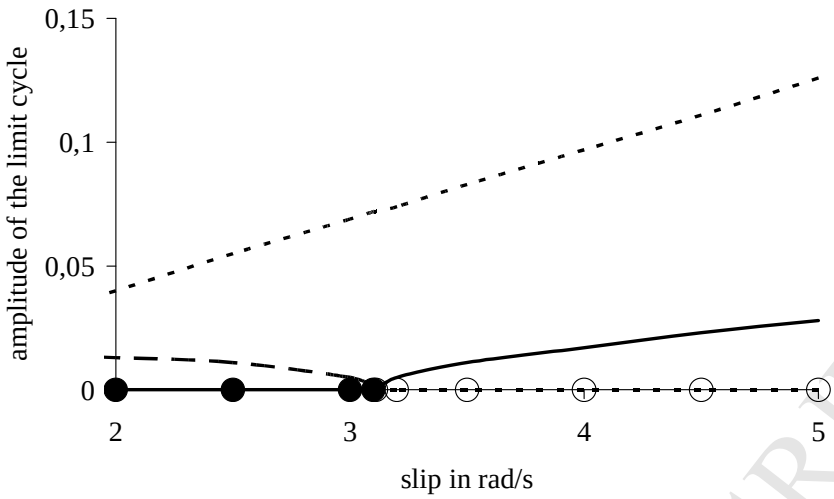

Fig. 7. Transcritical bifurcation in the disc's dynamics; stable equilibrium – solid line with solid dots, unstable equilibrium – dotted line with circles, stable periodic solution – solid line, unstable branch of the same periodic solution – dashed line, unstable periodic solution – dotted black line.

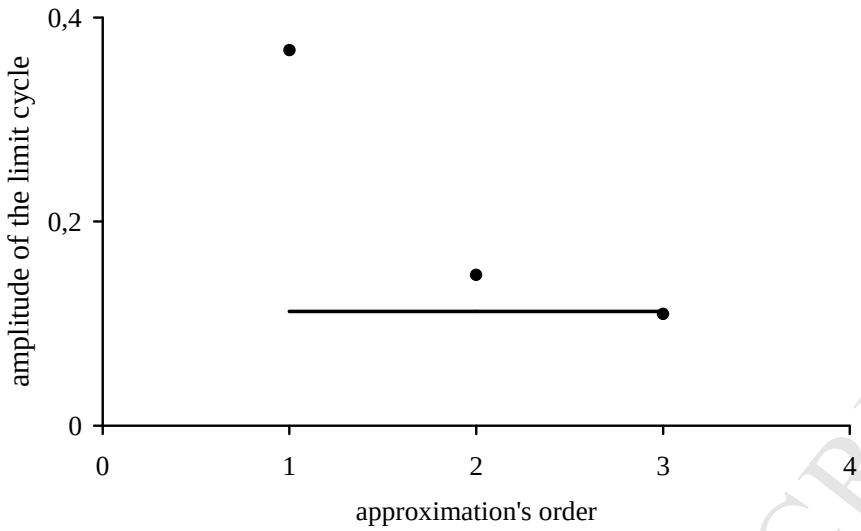

Fig. 8. Convergence of the analytic approximation (dots) to the numeric results (solid line)

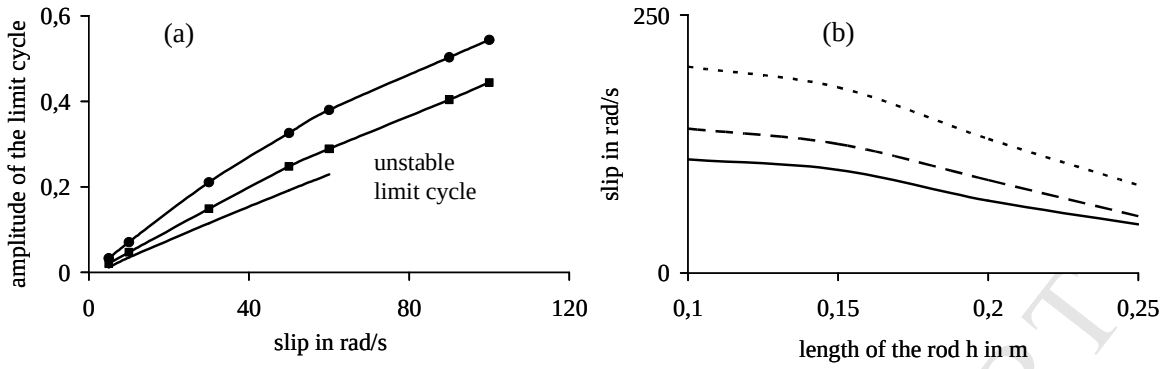

Fig. 9. Limit cycle and its stability domain; (a): h=0,1 for the line with circles, h=0,15 for the solid line with crosses, h=0,2 for the solid line; (b): $\omega = 100\,rad/s$ for the solid line, $\omega = 200\,rad/s$ for the dashed line, $\omega = 300\,rad/s$ for the dotted line